



Contents lists available at ScienceDirect

Thin Solid Films

journal homepage: www.elsevier.com/locate/tsf

Chemical bath deposition route for the synthesis of ultra-thin $\text{CuIn}(\text{S,Se})_2$ based solar cells

S. Lugo^a, Y. Sánchez^b, M. Neuschitzer^b, H. Xie^b, C. Insignares-Cuello^b, V. Izquierdo-Roca^b, Y. Peña^a, E. Saucedo^{b,*}

^a Universidad Autónoma de Nuevo León (UANL), Fac. de Ciencias Químicas, Av. Universidad S/N, Ciudad Universitaria, San Nicolás de los Garza, Nuevo León C.P. 66451, Mexico

^b Catalonia Institute for Energy Research (IREC), Jardins de les Dones de Negre 1, 08930 Sant Adrià del Besòs, Barcelona, Spain

ARTICLE INFO

Available online xxxx

Keywords:

Copper indium sulfoselenide
Indium sulfide
Copper sulfide
Chemical bath deposition
Raman spectroscopy
Thin films
Solar cells

ABSTRACT

$\text{CuIn}(\text{S,Se})_2$ (CISSe) photovoltaic grade thin films are usually grown by expensive vacuum based methods or chemical routes that require highly toxic precursors. In this work, we present the synthesis of CISSe absorbers by a simple chemical bath deposition (CBD) route. In the first step, $\text{In}_2\text{S}_3/\text{Cu}_2 - \text{xS}$ stack was deposited as a precursor by CBD on Mo-coated soda lime glass substrates, using respectively thioacetamide and *N,N'*-dimethylthiourea as S source. Then the CISSe thin films were synthesized by the precursor's selenization at 450 °C. The obtained films were characterized by X-ray diffraction (XRD), Raman spectroscopy and scanning electron microscopy (SEM). The tetragonal chalcopyrite structure of CISSe was identified by XRD and Raman, confirming that the major part of S was replaced by Se. SEM images show a compact and homogeneous film and by cross-section the thickness was estimated to be around 700 nm. Solar cells prepared with these absorbers exhibit an open circuit voltage of 369 mV, a short circuit current density of 13.7 mA/cm^2 , a fill factor of 45% and an efficiency of 2.3%.

© 2014 Published by Elsevier B.V.

1. Introduction

I–III–VI group compounds are among the leading light-absorbing semiconductors for thin film solar cells, with record efficiencies exceeding 20% at laboratory scale and 15% at module scale [1]. Among them, copper indium sulfur-selenide ($\text{CuIn}(\text{S,Se})_2$ —CISSe) has been one of the most promising photovoltaic materials because of its optical and electrical properties. It has a direct band gap between 1.0 and 1.5 eV depending on S/Se ratio and an absorption coefficient exceeding 10^5 cm^{-1} in the terrestrial solar spectrum range, which are ideal for the fabrication of thin film photovoltaic devices [2–4]. Although the band gap of this material is not in the optimal range defined by the Shockley–Queisser limit, CISSe is a very interesting material for applications that require high currents or as bottom cell in tandem concepts [5].

CISSe thin films have been deposited by several techniques including electrodeposition [6], electron beam evaporation [7], sputtering [8], and chemical bath deposition (CBD) [4,9]. Efficiencies between 9 and 11% have been reported using chemical based methods like particulate printing processes, electrodeposition or hydrazine based methods [10]. Nevertheless, these processes involve both toxic and hazardous precursors and/or complex synthesis methodologies. On the contrary, CBD is a simple and low cost method that produces uniform, adherent, and reproducible large area thin films, and has been spotlighted as an alternative to these methods, due to their potential to realize low cost PV devices [11].

Few studies reported solar cells using the CBD technique. Vidyadharan et al. [12] first reported the synthesis of CuInSe_2 and its incorporation in a cell by the CBD technique on a single deposit, obtaining a device with a maximum efficiency of 3.1%. Additionally, K. C. Rathod et al. [13] deposited CuInSe_2 layers by CBD, incorporating it in a photoelectrochemical cell, obtaining an efficiency of 0.82%.

In this study, we present a different approach for the synthesis of selenium rich CISSe films by depositing $\text{In}_2\text{S}_3/\text{Cu}_2 - \text{xS}$ stacked layers by CBD on SLG/Mo substrates, followed by a reactive annealing under Se atmosphere. The advantage of the multi-stack precursor is that it allows for an accurate control of the cationic composition of CISSe by simply varying the In_2S_3 and $\text{Cu}_2 - \text{xS}$ thicknesses. Using this approach a solar cell with 2.3% maximum efficiency is reported, encouraging the future development of this very low cost technology.

2. Experimental section

CISSe layers were synthesized using a two stage process: deposition of $\text{In}_2\text{S}_3/\text{Cu}_2 - \text{xS}$ stacked layers with a further annealing under Se atmosphere in a graphite box. In the first step, the deposition of the indium sulfide thin films was carried out on Mo-coated soda lime glass (SLG) substrates (800 nm in thicknesses, $0.16 \Omega/\square$). The composition of the chemical bath solution is: $\text{In}(\text{NO}_3)_3$ (99.9%, Aldrich) 0.1 M, CH_3COOH 0.5 M and CH_3CSNH_2 (99%, Aldrich) 1 M at a pH of 2.0 that was adjusted by adding diluted HCl; the final volume was adjusted to 100 mL with deionized water (18 M Ω). The chemical reaction was carried out at 55 °C

* Corresponding author.
E-mail address: esaucedo@irec.cat (E. Saucedo).

for 3 h and 45 min under continuous stirring, resulting in a layer with 380 nm in thickness. Then, during the second step $\text{Cu}_2 - \text{xS}$ layers were deposited on the $\text{In}_2\text{S}_3/\text{Mo}/\text{SLG}$ substrate. The procedure given in Ref. [14] was followed to deposit copper sulfide thin films by using $\text{CuCl}_2 \cdot 2\text{H}_2\text{O}$ (99%, Aldrich) 0.5 M, $\text{Na}_2\text{S}_2\text{O}_3$ (98%, Aldrich) 1 M, and N,N' -dimethylthiourea (99%, Aldrich) 0.5 M, with a final volume of 100 mL. These chemical reagents are typically used in CBD processes for the growth of different materials, and although some of them contain organic molecules, C contamination is not expected. The chemical reaction was carried out at 70 °C for 1 h and 35 min under continuous stirring, resulting in a film of 250 nm in thickness. The selected thicknesses correspond to Cu-rich conditions, in particular to a Cu/In ratio equal to 1.24. Cu-rich condition was selected because it promotes grain growth during the selenization process, although other compositions (in particular stoichiometric or Cu-poor) could be interesting for the optimization of the solar cell performance.

Finally, the CISSe thin films were synthesized by the selenization of the $\text{In}_2\text{S}_3/\text{Cu}_2 - \text{xS}$ stack precursors in a tubular furnace, using a graphite box with a volume of 23.5 cm³, containing 20 mg of Se powder with a total pressure of 1 bar under Ar atmosphere. The system was heated at 20 °C/min up to 450 °C for 30 min, and then naturally cooled down. The total process takes approximately 120 min.

The structural properties of the obtained films were analyzed by X-ray diffraction (XRD) using an X-ray diffractometer Siemens D-500 in θ - 2θ configuration (Cu K_α radiation, $\lambda = 1.5418$ Å). The surface morphology and film grain size were analyzed by scanning electron microscopy (SEM, FEI NovaTM NanoSEM 230) using a work distance of 5 mm and an operating voltage of 5 kV. The thin films obtained were also characterized by Raman spectroscopy in backscattering configuration using a Raman probe developed at the Catalonia Institute for Energy Research, coupled with an optical fiber to an iHR320 Horiba Jovin Yvon spectrometer. In order to optimize the signal of the secondary phases present in the layer, the Raman characterization has been performed under 532 nm and 785 nm excitation wavelengths. In both excitation wavelengths the optimal excitation power density has been studied in order to avoid the thermal effect in the measurements. All measurements have been calibrated fixing the 520 cm⁻¹ Raman shift for the main mode of the Si monocrystal spectrum.

For the solar cells, absorbers were etched with a KCN solution (5% w/V, 2 min), CdS buffer layer (~60 nm) was deposited by CBD, and intrinsic ZnO and ZnO:Al films were grown by pulsed direct current magnetron sputtering deposition (CT100 Alliance Concepts). For the optoelectronic characterization, 3×3 mm² cells were scribed using a micro-diamond scribe (MR200 OEG). Measurement of the optoelectronic properties was carried out using a pre-calibrated Sun 3000 Class AAA solar simulator from Abet Technologies (uniform illumination area of 15×15 cm², AM 1.5 filter) and the external quantum efficiency (EQE) of the devices was also measured, using a Bentham PVE300 system.

3. Results and discussion

XRD diffractograms are shown in Fig. 1, including the as deposited $\text{In}_2\text{S}_3/\text{Cu}_2 - \text{xS}$ layers (a) and the as annealed CISSe layer (b). The diffractogram of the as deposited $\text{In}_2\text{S}_3/\text{Cu}_2 - \text{xS}$ precursor layer is dominated for the diffraction peaks corresponding to Mo (JCPDS file 042-1120). Additionally, broad and weak peaks at 28.4°, 33.6° and 48.2°, and a shoulder at 29.4° can be observed. These contributions are assigned to In_2S_3 [15] and $\text{Cu}_2 - \text{xS}$ (JCPDS file 29-6578) phases. The weak intensity of these peaks and their high full width at half maximum (FWHM) indicate the amorphous nature of the precursors. After the selenization of the $\text{In}_2\text{S}_3/\text{Cu}_2 - \text{xS}$ precursors, the crystal structure of the resulting polycrystalline CISSe thin films correspond to the tetragonal chalcopyrite phase (JCPDS 040-1487), with a $[\text{S}]/([\text{S}] + [\text{Se}])$ ratio of 0.08, estimated by the Vegard's law [16]. This suggests that during the annealing process, almost all the S was substituted by Se, leading to a Se rich CISSe chalcopyrite phase. The symmetry of the CISSe diffraction

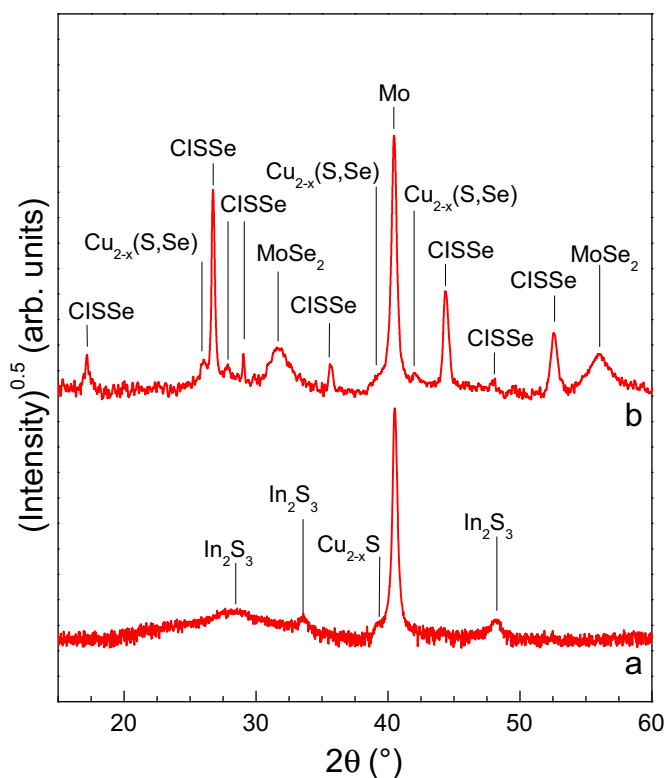


Fig. 1. XRD diffractograms: a) as-deposited $\text{In}_2\text{S}_3/\text{Cu}_2 - \text{xS}$ multi-stack precursor, and b) absorber selenized at 450 °C/30 min.

peaks and their low FWHM (FWHM = 0.26° from (112) at 24.75°) suggest a high crystalline quality absorber and constant CISSe in depth composition. Additionally, a weak contributions at 29.0° and 42.0° and a shoulder centered at 39.2° could be identified with diffraction peaks corresponding to the $\text{Cu}_2 - \text{x}(\text{S,Se})$ alloy. The formation of this phase is in agreement with the Cu-rich composition of the precursor. This Cu-rich phase act as crystallization flux, facilitating the grain growth and allowing obtaining large grain layers [17]. Also, peaks at 31.7° and 56.0° are assigned to MoSe_2 (JCPDS 29-0914), demonstrating that Mo was partially selenized during the annealing process. This confirms that the methodology proposed in this paper is useful for the synthesis of Se rich CISSe chalcopyrite layers from the selenization of Cu and In sulfide precursors deposited by CBD.

In Fig. 2a the top view of $\text{Cu}_2 - \text{xS}$ layer is presented, where nanometric scale needles are observed. The cross section view of the stacked precursor (Fig. 2b) supports the amorphous like nature of the bi-layer, presenting a very fine grain structure. After selenization, the morphology of the surface changes drastically (Fig. 2c to f). Larger grains are observed in the surface (around 200 nm) confirming the adequate crystallization of the material. Also, hexagonal platelets are clearly seen on top (see Fig. 2c), which are typically associated with $\text{Cu}_2 - \text{xSe}$ and/or $\text{Cu}_2 - \text{xS}$, confirming the presence of Cu-rich secondary phases. Using the cross sectional views of the absorber we can estimate a thickness of 740 nm approximately (Fig. 2d), with a very thin MoSe_2 layer (less than 50 nm), confirming the good crystallization of the precursor, and demonstrating the potentiality of this approach to produce layers with large grain structure. After KCN etching (Fig. 2e and f for top and cross sectional views respectively), the hexagonal platelets are effectively removed from the surface, supporting that these overgrowths are Cu-chalcogenide binary phases. Additionally, the surface is clearly smooth when compared with the as annealed absorber, being this etching effect beneficial for the hetero-junction properties.

In Fig. 3 the Raman spectra of the as grown In_2S_3 (spectra a1 and b1), $\text{In}_2\text{S}_3/\text{Cu}_2 - \text{xS}$ stacked layers (spectra a2 and b2), and the corresponding

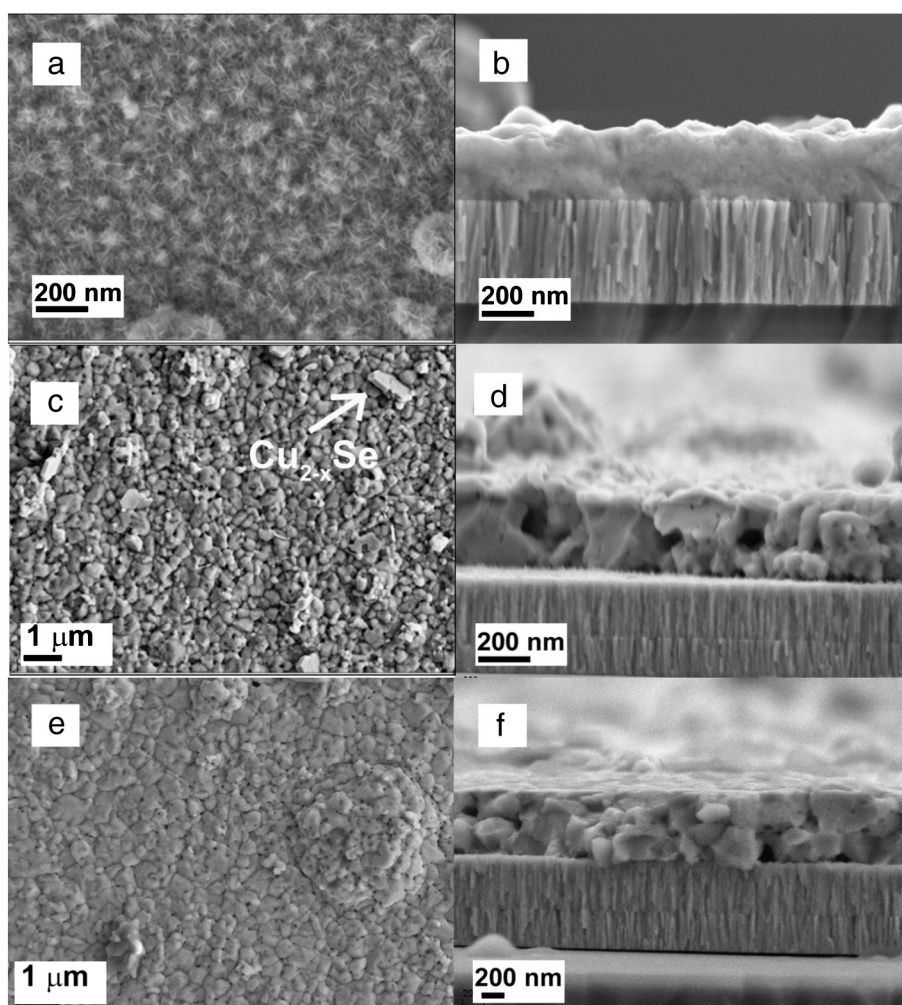


Fig. 2. SEM top (a) and cross sectional (b) views of the as-prepared precursors, top (c) and cross sectional (d) views of the as annealed one, and top (e) and cross sectional (f) views of the as etched layers using a KCN solution.

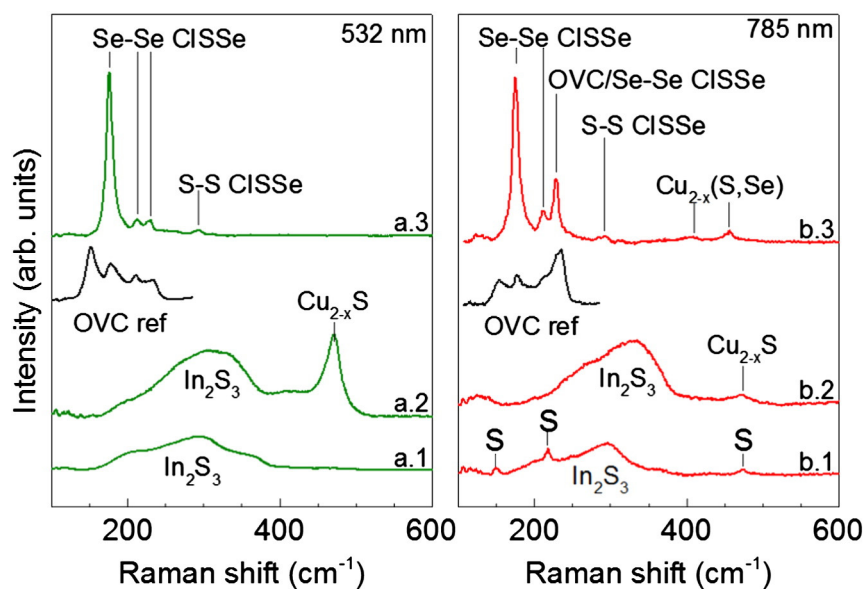


Fig. 3. Raman spectra of In_2S_3 (a1–b1), $\text{In}_2\text{S}_3/\text{Cu}_{2-x}\text{S}$ (a2–b2) and $\text{CuIn}(\text{S,Se})_2$ (a3–b3) under 532 nm and 785 nm excitation wavelengths. Also the reference spectra of OVC phase is included (spectra in black color).

absorber after selenization (spectra a3 and b3), using 532 nm and 785 nm are presented. The penetration depth under both excitation wavelengths is estimated below 100 nm providing information from the sample surface. The a1 and b1 Raman spectra are characterized by a broad band in the region of 150–400 cm^{-1} . The detection of this band confirms the formation of amorphous like In_2S_3 [18]. Additionally under a 785 nm excitation wavelength a small contribution identified with elemental sulfur is observed [19]. The presence of this signal suggests the precipitation of rather small quantities of sulfur during the growth of In_2S_3 . In the spectra corresponding to the $\text{In}_2\text{S}_3/\text{Cu}_2 - \text{xS}$ stack (a2 and b2) the broad band assigned to amorphous like In_2S_3 is clearly modified, with changes in the shape and ratios between the different contributions, suggestion and improvement of the crystalline quality [18]. This crystallization could be associated with the high temperatures used for the chemical bath deposition of $\text{Cu}_2 - \text{xS}$. Additionally, a weak contribution at 473 cm^{-1} identified as $\text{Cu}_2 - \text{xS}$ phase is detected [20]. From the Raman analysis, there are no clear evidences of the inter-mixing between Cu sulfide and In sulfide precursors, with the concomitant formation of CuInS_2 or related phases. It is important to remark that the In_2S_3 Raman signal is also observed in the spectra a2 and b2 because the upmost $\text{Cu}_2 - \text{xS}$ layer is very porous (as is clearly observed in Fig. 2a), and is not enough to cover completely the In_2S_3 bottom layer.

After the selenization of this precursor, the Raman spectrum with green excitation (a3) shows a main peak at 176 cm^{-1} , with three weaker contributions at 212 cm^{-1} , 228 cm^{-1} and 290 cm^{-1} . The low FWHM of the main A1 mode (10 cm^{-1} , in this system the FWHM of the 520 cm^{-1} mode of crystalline Si used as reference is 6.4 cm^{-1}) confirms the high crystalline quality of the absorber. These contributions are assigned to very Se-rich $\text{CuIn}(\text{S,Se})_2$ chalcopyrite phase (with more than 90% of Se) [21], in close agreement with the XRD analysis. Using a 785 nm excitation wavelength, two additional features are observed in the 390–475 cm^{-1} frequency region, and are tentatively assigned to sulfur rich $\text{Cu}_2 - \text{x}(\text{S,Se})$ [22,23]. The formation of this phase is in agreement with the Cu-rich composition of the precursor. Additionally, the intensity of the 228 cm^{-1} mode increases (see spectrum b3) under 785 nm excitation. Under this condition, the increase of this contribution is assigned to the presence of Ordered Vacancy Compound (OVC) phases, as is illustrated in the OVC reference spectra (corresponding to CuIn_3Se_5) in the same figure [24]. Differences between the reference and the absorber spectra correspond to different OVC compositions (OVC phases have several stoichiometries including CuIn_5Se_8 , $\text{CuIn}_2\text{Se}_{3.5}$, and $\text{CuIn}_{1.5}\text{Se}_2$) [24,25]. Although the OVC phases are usually associated with Cu-poor conditions, it was reported that these phases can be also formed close to Cu–Se secondary phases in Cu-rich layers, as those observed in Fig. 2a [17]. In this case, the grains in contact with the Cu–Se binary phase can be Cu-poor (although the overall composition of the layer is Cu-rich), explaining the unexpected presence of OVC phases in Cu-rich layers.

To confirm the potential of the absorbers produced by the two stage process, CISse layers obtained from the selenization of $\text{In}_2\text{S}_3/\text{Cu}_2\text{S}$ stacks at 450 °C/30 min were tested as absorber materials in solar cells. Fig. 4a shows the obtained current density–voltage (J–V) curve for the best cell, where the following optoelectronic parameters were extracted: open circuit voltage, $V_{oc} = 369$ mV; short circuit current density, $J_{sc} = 13.7$ mA/cm^2 ; fill factor, $FF = 45\%$; and efficiency of 2.3%. The V_{oc} is only slightly lower than those reported in literature for the best CISse solar cells [10], suggesting that the absorber has a good quality, as was demonstrated before using Raman spectroscopy. Also, the presence of OVC's in the surface detected by this technique (see Fig. 3b) could contribute to the reduction of the density of defects [25,26], enhancing the cell's voltage. Nevertheless, the J_{sc} and FF of the cell are remarkably lower than values expected for this material [27,28]. The low current could be related, at least in part, to the thinner absorber which is only 700 nm in thickness with respect to typical 1.5–2.0 μm used in this technology. The low FF can be explained by the low shunt and high series

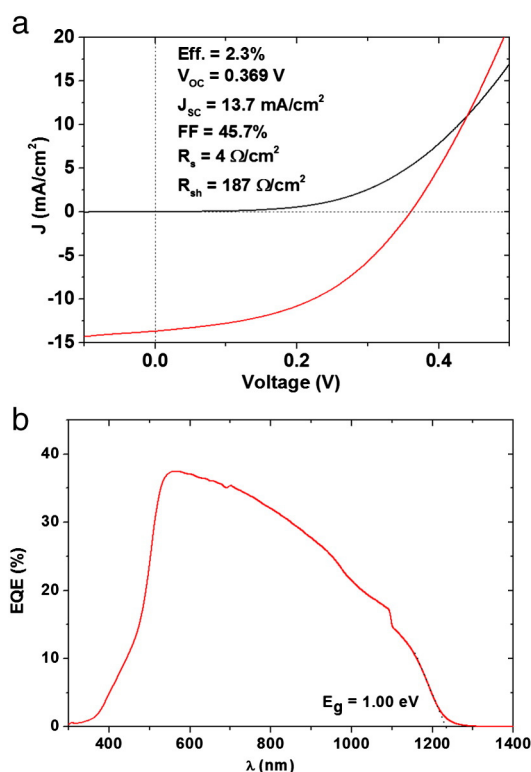


Fig. 4. J–V illuminated and dark curves of the best cell obtained in this work (a) and corresponding EQE (b).

resistance characteristics of this device that could be related to the Cu-rich conditions employed in this work (and the concomitant formation of Cu–Se binary phases). Additionally, no optimized junction and/or electrical contacts could be the reason of these low values. Finally, the voids observed in Fig. 2b are also contributing to the deterioration of the current of the cell. The external quantum efficiency (EQE %) spectrum for the CISse thin film solar cell is shown in Fig. 4b. The maximum value of the EQE is around 40%, confirming the non-optimized charge carrier collection, which origin is under study to improve the solar cell characteristics. Using the high wavelength region of the EQE we estimate a band gap of the material equal to 1.0 eV, in agreement with XRD and Raman spectroscopy, where Se-rich CISse absorber was observed. Nevertheless, although the efficiency of the devices presented here is considered low, the technique has potentiality to produce a photovoltaic grade material. Future improvements in the cationic composition (Cu/In ratio), modifications in the bath conditions to increase the deposition rate, optimization of the annealing parameters, passivation of the rear contact, etc., will be a pre-requisite to increase the efficiency.

In summary, CISse based thin film solar cells obtained in this work by the CBD technique are viable for low cost concepts for the synthesis of ultra thin Se-rich CISse absorbers. However, there are many aspects to be considered in the future for increasing the efficiency of these devices. An interesting alternative is to use a passivation layer formed by $\text{MgF}_2/\text{Al}_2\text{O}_3$, as was reported by B. Vermang et al. [28], to increase the V_{oc} and J_{sc} and consequently the device efficiency.

4. Conclusions

$\text{CuIn}(\text{S,Se})_2$ ultra-thin films were prepared on Mo/SLG, by means the selenization of chemically deposited $\text{In}_2\text{S}_3/\text{Cu}_2 - \text{xS}$ stacked layers. The structural, morphological and optical properties of precursors as well as absorbers were investigated. XRD and Raman spectroscopy show that the precursor is formed by amorphous like In_2S_3 and $\text{Cu}_2 - \text{xS}$ binary phases, with rather marginal mixing between them. After selenization, Se-rich $\text{CuIn}(\text{S,Se})_2$ layers with large grains, tetragonal

chalcopyrite structure and approximately 700 nm in thickness were obtained, with $\text{Cu}_2 - x(\text{S},\text{Se})$ binary compound as the secondary phase. Solar cells prepared with this absorber exhibit a maximum conversion efficiency of 2.3%, with 369 mV of V_{oc} , 13.7 mA/cm² of J_{sc} and 45% of FF. In summary, the possibility to synthesize photovoltaic grade Se-rich CISse absorbers by a two step CBD technique is demonstrated.

Acknowledgments

The research leading to these results has received funding from the People Program (Marie Curie Actions) of the European Union's Seventh Framework Program FP7/2007–2013/ under REA grant agreement No. 316488 (KESTCELLS) and No. 285897 (INDUCIS), by European Regional Development Funds (ERDF, FEDER Programa Competitivitat de Catalunya 2007–2013), and CONACyT project No. 178228 and Laboratory Research and Technological Development 2009 No. 124177. Authors from IREC and IN2UB belong to the M-2E (Electronic Materials for Energy) Consolidated Research Group and the XarMAE Network of Excellence on Materials for Energy of the “Generalitat de Catalunya”. Y.S. thanks the PTA fellowship (PTA2012-7852-A), H.X. the “China Scholarship Council” fellowship (CSC No. 201206340113), V.I. the “Juan de la Cierva” fellowship (JCI-2011-10782) and E.S. the “Ramon y Cajal” fellowship (RYC-2011-09212).

References

- [1] M.A. Green, K. Emery, Y. Hishikawa, W. Warta, E.D. Dunlop, Solar cell efficiency tables (version 43), *Prog. Photovolt. Res. Appl.* 22 (2014) 1.
- [2] H. Liu, Z. Jin, J. Wang, J. Ao, G. Li, Well-dispersed CuInSe_2 nanoplates and nanoplates-ink-coated thin films for photovoltaic application by a triethylene glycol based solution process, *Mater. Lett.* 94 (2013) 1.
- [3] C.R. Kim, S.Y. Han, C.H. Chang, T.J. Lee, S.O. Ryu, Synthesis and characterization of CuInSe_2 thin films for photovoltaic cells by a solution-based deposition method, *Curr. Appl. Phys.* 10 (2010) S383.
- [4] P.P. Hankare, K.C. Rathod, P.A. Chate, A.V. Jadhav, I.S. Mulla, Preparation and characterization of CuInSe_2 thin films by chemical bath deposition technique, *J. Alloys Compd.* 500 (2010) 78.
- [5] Z. Jehl-Li-Kao, T. Kobayashi, T. Nakada, $\text{CuIn}(\text{Se}_{1-x}\text{Te}_x)_2$ solar cells with tunable narrow-bandgap for bottom cell application in multijunction photovoltaic devices, *Energy Mater. Sol. Cells* 119 (2013) 144.
- [6] S. Hamrouni, M.S. Alkhalifah, M.F. Boujmil, K. Ben Saad, Preparation and characterization of CuInSe_2 electrodeposited thin films annealed in vacuum, *Appl. Surf. Sci.* 292 (2014) 231.
- [7] H. Abdullah, S. Habibi, Effect of annealing temperature on $\text{CuInSe}_2/\text{ZnS}$ thin-film solar cells fabricated by using electron beam evaporation, *Int. J. Photoenergy* 2013 (2013) 568904.
- [8] M. Oertel, T. Hahn, H. Metzner, W. Witthuhn, CuInSe_2 solar cells by sequential absorber layer processing, *Phys. Status Solidi C* 6 (2009) 1253.
- [9] C.-H. Wu, J.-S. Ma, S.-H. Lin, C.-H. Lu, Synthesis of CuInSe_2 thin films on flexible Ti foils via the hydrothermally-assisted chemical bath deposition process at low temperatures, *Sol. Energy Mater. Sol. Cells* 112 (2013) 47.
- [10] C.J. Hibberd, E. Chassaing, W. Liu, D.B. Mitzi, D. Lincot, A.N. Tiwari, Non-vacuum methods for formation of $\text{Cu}(\text{In}, \text{Ga})(\text{S}, \text{Se})_2$ thin film photovoltaic absorbers, *Prog. Photovolt. Res. Appl.* 18 (2010) 434.
- [11] M.D. Mahanubhav, V.R. Patil, P.K. Khanna, Studies on chemically deposited CuInSe_2 thin films, *Mater. Lett.* 61 (2007) 2058.
- [12] P.K. Vidyadharan Pillai, K.P. Vijayakumar, Characterization of CuInSe_2 CdS thin-film solar cells prepared using CBD, *Sol. Energy Mater. Sol. Cells* 51 (1998) 47.
- [13] K.C. Rathod, P.A. Chate, K.M. Garadkar, D.J. Sathe, I.S. Mulla, Chemical deposition of CuInSe_2 thin films by photoelectrochemical applications, *J. Alloys Compd.* 511 (2012) 50.
- [14] M.T.S. Nair, Laura Guerrero, P.K. Nair, Conversion of chemically deposited CuS thin films to $\text{Cu}_{1.8}\text{S}$ and $\text{Cu}_{1.96}\text{S}$ by annealing, *Semicond. Sci. Technol.* 13 (1998) 1164.
- [15] P. Pistor, R. Caballero, D. Hariskos, V. Izquierdo-Roca, R. Wa, S. Schorr, R. Klenk, Quality and stability of compound indium sulphide as source material for buffer layers in $\text{Cu}(\text{In}, \text{Ga})\text{Se}_2$ solar cells, *Sol. Energy Mater. Sol. Cells* 93 (2009) 148.
- [16] A.R. Denton, N.W. Ashcroft, Vegard's law, *Phys. Rev. A* 43-6 (1991) 3161.
- [17] E. Saucedo, V. Izquierdo-Roca, C.M. Ruiz, L. Parissi, C. Broussillou, P.-P. Grand, J.S. Jaime-Ferrer, A. Pérez-Rodríguez, J.R. Morante, V. Bermúdez, Key role of Cu–Se binary phases in electrodeposited CuInSe_2 precursors on final distribution of Cu–S phases in $\text{CuIn}(\text{S}, \text{Se})_2$ absorbers, *Thin Solid Films* 517 (2009) 2268.
- [18] B. Asenjo, C. Guillén, A.M. Chaparro, E. Saucedo, V. Bermúdez, D. Lincot, J. Herrero, M.T. Gutiérrez, Properties of In_2S_3 thin films deposited on ITO/glass substrates by chemical bath deposition, *J. Phys. Chem. Solids* 71 (2010) 1629.
- [19] A.T. Ward, Raman spectroscopy of sulfur, sulfur–selenium, and sulfur–arsenic mixtures, *J. Phys. Chem.* 72 (1968) 4133.
- [20] P. Kumar, M. Gusain, R. Nagarajan, Synthesis of $\text{Cu}_{1.8}\text{S}$ and CuS from copper–thiourea containing precursors; anionic (Cl^- , NO_3^- , SO_4^{2-}) influence on the product stoichiometry, *Inorg. Chem.* 50 (2011) 3065.
- [21] V. Izquierdo-Roca, X. Fontané, J. Álvarez-García, L. Calvo-Barrio, A. Pérez-Rodríguez, J.R. Morante, C.M. Ruiz, E. Saucedo, V. Bermúdez, Electrochemical synthesis of $\text{CuIn}(\text{S}, \text{Se})_2$ alloys with graded composition for high efficiency solar cells, *Appl. Phys. Lett.* 94 (2009) 061915.
- [22] I. Motohiko, K. Shibata, H. Nozaki, Anion distributions and phase transitions in $\text{CuS}_{1-x}\text{Se}_x$ ($x = 0-1$) studied by Raman spectroscopy, *J. Solid State Chem.* 105 (1993) 504.
- [23] V. Izquierdo-Roca, A. Pérez-Rodríguez, A. Romano-Rodríguez, J.R. Morante, J. Álvarez-García, L. Calvo-Barrio, V. Bermúdez, P.P. Grand, O. Ramdani, L. Parissi, O. Kerrec, Raman microprobe characterization of electrodeposited S-rich $\text{CuIn}(\text{S}, \text{Se})_2$ for photovoltaic applications: microstructural analysis, *J. Appl. Phys.* 101 (2007) 103517.
- [24] C.-M. Xu, X.-L. Xu, J. Xu, X.-J. Yang, J. Zuo, N. Kong, W.-H. Huang, H.-T. Liu, Composition dependence of the Raman A_1 mode and additional mode in tetragonal Cu-In-Se thin films, *Semicond. Sci. Technol.* 19 (2004) 1201.
- [25] C. Insignares-Cuello, C. Broussillou, V. Bermúdez, E. Saucedo, A. Pérez-Rodríguez, V. Izquierdo-Roca, Raman scattering analysis of electrodeposited $\text{Cu}(\text{In}, \text{Ga})\text{Se}_2$ solar cells: impact of ordered vacancy compounds on cell efficiency, *Appl. Phys. Lett.* 105 (2014) 021905; C.M. Ruiz, X. Fontané, A. Fairbrother, V. Izquierdo-Roca, C. Broussillou, S. Bodnar, A. Pérez-Rodríguez, V. Bermúdez, Impact of electronic defects on the Raman spectra from electrodeposited $\text{Cu}(\text{In}, \text{Ga})\text{Se}_2$ solar cells: application for non-destructive defect assessment, *Appl. Phys. Lett.* 102 (2013) 091106.
- [26] S. Siebentritt, L. Gütay, D. Regesch, Y. Aida, V. Deprédurand, Why do we make $\text{Cu}(\text{In}, \text{Ga})\text{Se}_2$ solar cells non-stoichiometric? *Sol. Energy Mater. Sol. Cells* 119 (2013) 18.
- [27] J. Song, S.S. Li, C.H. Huang, O.D. Crisalle, T.J. Anderson, Device modeling and simulation of the performance of $\text{Cu}(\text{In}_{1-x}\text{Ga}_x)\text{Se}_2$ solar cells, *Solid State Electron.* 48 (2004) 73.
- [28] Bart Vermang, Jörn Timo Wätjen, Viktor Fjällström, Fredrik Rostvall, Marika Edoff, Ratan Kotipalli, Frederic Henry, Denis Flandre, Employing Si solar cell technology to increase efficiency of ultra-thin $\text{Cu}(\text{In}, \text{Ga})\text{Se}_2$ solar cells, *Prog. Photovolt. Res. Appl.* (2014), <http://dx.doi.org/10.1002/pip.2527>.